URSI GASS 2021, Rome, Italy, 28 August - 4 September 2021

A Gain Enhanced Metasurface based Monopole Antenna for WLAN Application

Diptiranjan Samantaray, and Somak Bhattacharyya
Department of Electronics Engineering, IIT (BHU), Varanasi, Uttar Pradesh, 221005

Abstract

The design and performance of a highly directive gain enhanced metasurface antenna (MSA) has been reported in this paper. The MSA is formed by incorporating the T-shaped patch with 3×5 order metasurface (MS) in which the MS is associated with annular hexagonal shaped patches arranging in periodic manner. This antenna operates at 4.99 GHz and the -10 dB impedance bandwidth has been achieved in the range 4.79 GHz-5.09 GHz. The antenna provides the maximum realized gain of 11.2 dBi at 4.99 GHz. The endfire radiation pattern has been observed along E-plane while nearly omnidirectional pattern has been realized along H-plane. The designed structure can be promoted for WLAN applications.

1. Introduction

Recently, highly directive gain enhanced planar antennas are more challenging due to their ease of fabrication and low profile [1-8]. Furthermore, these type of special antennas are lighter than conventional reflector antenna and easier to install [6-10]. Various metasurface-embedded designs have been reported in past few years giving rise to highly directive radiation pattern at the far field characteristics [8-12]. The devices such as artificial magnetic conductors (AMC), high impedance surfaces and electromagnetic bandgap (EBG) structures have been reported by utilizing the properties of the metasurface (MS) [5-12]. The key features of MS are low complexity with beam control capability in terms of shaping, pointing and scanning along with implementation amenable to very different technologies [10-17]. Low mass, low envelope, high gain, directive and low power losses are important features of any MS design [5-10]. Owing to these, they have set up applications in various domains such as wireless broadcasting, satellite communication and medical applications [2-8]. MS structures exhibit flexible reflection characteristics and manageable dispersion properties either in the form of surface or guided waves in addition to several applications like absorber, polarization conversion etc. [18-19].

In this manuscript, a high gain and directive MS antenna has been designed. Here, the proposed antenna integrates with a T-shaped monopole and a 3×5 order MS containing annular hexagonal shaped patches arranged in periodic manner. The proposed MS antenna works at 4.99 GHz with fractional bandwidth of 6.21%. This prototype provides a return loss of 28 dB and the maximum realized gain of 11.2 dBi at 4.99 GHz. The proposed antenna exhibits endfire radiation pattern along E-plane while nearly omnidirectional pattern has realized along H-plane in its far-field characteristics.

2. Design of Metasurface Antenna

The proposed antenna assembles with a T-shaped monopole patch as a primary element and the 3×5 order MS. Here the monopole patch and the MS are designed in the same plane in which the primary T-shaped antenna follows the 3×5 order annular hexagonal patches. The 2D schematic views of the proposed structure have been represented in Figure 1 and the detailed parametrically optimized dimensions of the proposed structure are mentioned in Table 1. The antenna is excited by a 50Ω microstrip feedline applied with respect to the ground plane. The proposed antenna has been designed on FR4 dielectric (relative permittivity of 4.4 and loss tangent of 0.025) having thickness of 1.6 mm.

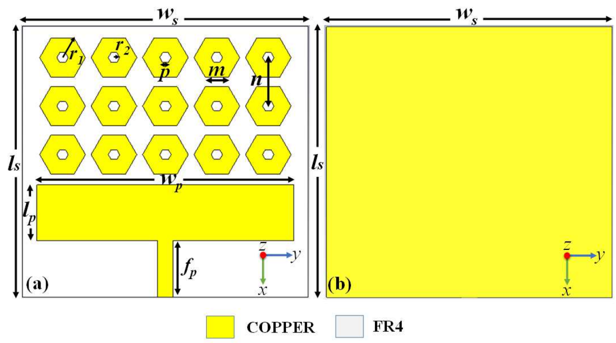

Figure 1. (a) Top view and (b) bottom view of the metasurface antenna

Table 1. The optimized geometrical parameters of the MS antenna

Optimized Parameters	Dimension (mm)	Optimized Parameters	Dimension (mm)
w_s	100	r_1	8
l_s	95	r_2	2
w_p	90	m	8
l_p	19.5	n	18
p	2	f_p	19.8

The top and bottom views of the conventional antenna shown in Figure 1(a) and Figure 1(b) are designed on FR4 dielectric with 100×95 mm^2 cross-section. Initially, a 90×19.5 mm^2 rectangular patch has been used as a radiating element. This monopole antenna operates at two frequency regions viz., 4.74-4.81 GHz and 4.94-5.12 GHz. In this case, both the bands are narrow and the maximum realized gain of 7.8 dBi has been achieved at 4.77 GHz. Later, these narrow bands have been enhanced into wideband by incorporating a 3×5 order MS along with the T-shaped patch. Here, the MS and the T-shaped monopole patch are designed in the same *xy*-plane. The annular hexagonal shaped unit cell is formed by optimizing the outer radius as 8 mm and the inner radius as 2 mm. Further, the dimension of the outer side of hexagonal patch has been optimized to 8 mm while the inner one as 2 mm. The 3D view of proposed unit cell is illustrated in Figure 2(a). The four sides of unit cell are set to be periodic boundaries whereas the top and bottom faces are assigned with ports. The unit cell is excited by periodic boundary conditions using commercial software CST Microwave Studio [20]. The basic electromagnetic behaviors of effective permittivity and permeability of the MS layer have been studied and analyzed. The real and imaginary parts of the same are illustrated in Figure 2(b) and Figure 2(c) respectively. The MS layer behaves as a left-handed material (LHM) in the frequency band 4.8-5.8 GHz.

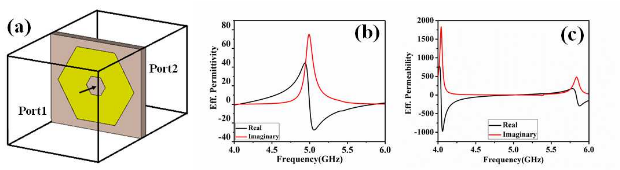

Figure 2. (a) The 3D view (b) Effective permittivity and (c) Effective permeability of unit cell.

The unit cells of the MS are arranged in such a way that, it follows the homogeneity properties of the metasurface. The incorporation of the MS layer just top of the T-shaped conventional patch improves the performance of the antenna. The designed antenna operates in the frequency band ranging from 4.79-5.10 GHz with the maximum fractional bandwidth of 6.21% and the realized gain of 11.2 dBi at 10.89 GHz. It is also observed that further increase of number of unit cells in the MS, the performance of the antenna gets enhanced.

3. Simulated Results

All the optimization and analyses of the proposed MS antenna have been performed using CST Microwave Studio 2017 [20]. The simulated -10 dB impedance bandwidth responses of the antenna with and without MS layer are provided in Figure 3. It is seen from Figure 3 that the conventional antenna operates in the frequency regions ranging from 4.74- 4.81 GHz and 4.94- 5.12 GHz with return loss of 25 dB at 5.04 GHz. Further, the integration of MS with the conventional antenna exhibits good impedance matching with S_{11} less than −28 dB at 4.99 GHz. The MS layer with T-shaped patch possess a good reflection coefficient at the optimized frequency band with the impedance bandwidth of 6.21%.

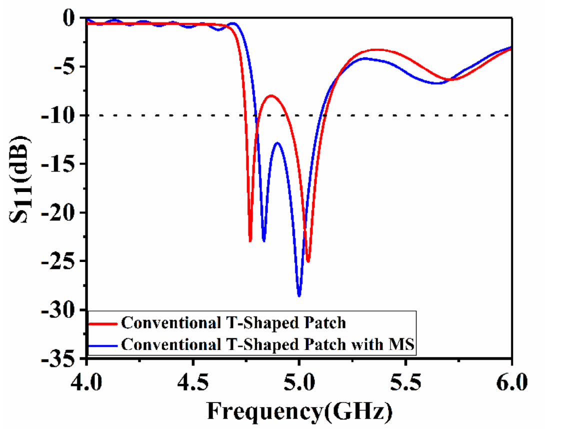

Figure 3. Plot of S_{11} (dB) with respect to frequency of the proposed antenna prototype.

The electric field distributions of the proposed structure at different operating frequencies have been shown in Figure 4. It is also observed that at 4.99 GHz the field distibution is maximum around the centre interface of the patch and the surface interface of the unit cells.

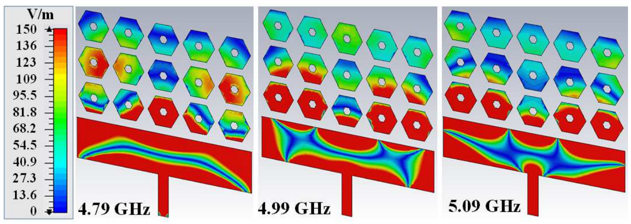

Figure 4. Electric field distributions of the proposed antenna structure at 4.79 GHz, 4.99 GHz and 5.09 GHz at different surfaces.

The surface current distributions at 4.79 GHz, 4.99 GHz and 5.09 GHz for top surface have been studied and shown in Figure 5. They are denser around the patch position of the conventional antenna and also the surface of unit cells. Also at 4.79 GHz the surface current moves from left to right whereas at 4.99 GHz and 5.09 GHz the surface current moves from right to left. It is evident from Figure 5 that at 4.99 GHz, the surface current is maximum; thereby realizing the best impedance matching.

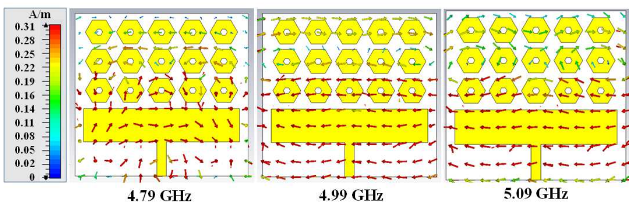

Figure 5. Surface current of the proposed prototype at 4.79 GHz, 4.99 GHz and 5.09 GHz.

The three-dimensional gain radiation patterns at different frequencies are studied in Figure 6. The proposed MS antenna provides the realized gains of 6.03 dBi, 11.2 dBi and 10.8 dBi at the respective operating frequencies of 4.79 GHz, 4.99 GHz and 5.09 GHz. Here, the 3D gain pattern is highly directed towards 0^{0} in all the bands and it is maximum at 4.99 GHz.

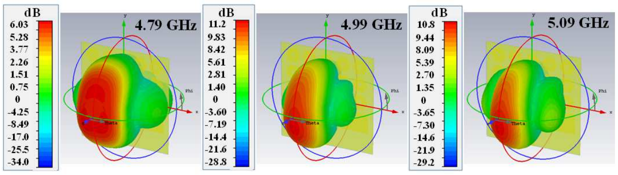

Figure 6. 3D radiation pattern of the proposed prototype at different operating frequencies of 4.79 GHz, 4.99 GHz and 5.09 GHz.

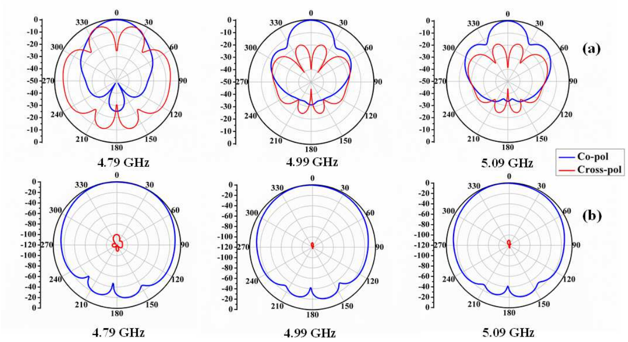

Figure 7. (a) E-plane and (b) H-plane co-polarized and cross-polarized radiation patterns at 4.79 GHz, 4.99 GHz and 5.09 GHz.

Table 2. A Comparative analysis of Proposed prototype with Exsiting Antennas

Antenna Literature	Operating Frequency (GHz)	Fractional Bandwidth (%)	Gain (dBi)	Radiating Element
Painam *et al.* [3]	6.22	4.5	4.13	Circular radiating patch
Saghanezhad *et al.* [4]	6.2	6.9	4.3	Patch Antenna
Xu *et al.* [5]	3.11	1.61	4.15	slot-loaded square patch
Liu *et al.* [6]	10.6	7.9	6.2	Rectangular patch antenna
Proposed Design	4.99	6.21	11.2	T-shaped patch

The complete analysis of co-polarized and cross-polarized radiation characteristics of the MS-based antenna at 4.79 GHz, 4.99 GHz and 5.09 GHz along E-plane and H-plane have been observed in Figure 7. Here, the endfire radiation characteristics have been observed along E-plane as the main lobe is directed towards 0^{0} in all the operating frequencies. Further, nearly omni-directional pattern has been noticed in the H-plane and the cross-polarized radiation level is much below than the co-polarized ones at all the operating frequencies.

A comparative study of previously reported MS type antenna structures have been carried out with the proposed one as provided in Table 2. It can be seen that the presented antenna achieves superior gain enhancement over the operating band in comparison to the reported ones.

4. Conclusion

In this paper, a highly directive gain enhanced MS antenna has been analyzed and studied. The proposed antenna operates over the frequency region 4.79-5.10 GHz with maximum impedance bandwidth of 6.21% at 4.99 GHz. The realized gain of 11.2 dBi has been achieved at 4.99 GHz due to incorporation of the MS. The antenna provides endfire radiation pattern along E-plane and nearly omnidirectional radiation pattern along H-plane. This antenna is applicable for WLAN applications.

5. References

1. A. Baba, R. M. Hashmi, K. P. Esselle, J. G. Marin and J. Hesselbarth, "Broadband Partially Reflecting Superstrate-Based Antenna for 60 GHz Applications," in *IEEE Transactions on Antennas and Propagation*, **67**, 7, July 2019, pp. 4854-4859, doi: 10.1109/TAP.2019.2916474.

2. W. E. I. Liu, Z. N. Chen, X. Qing, J. Shi and F. H. Lin, "Miniaturized Wideband Metasurface Antennas," in *IEEE Transactions on Antennas and Propagation*, **65**, 12, December 2017, pp. 7345-7349, doi: 10.1109/TAP. 2017.2761550.

3. S. Painam, and B. Chandramohan. “Miniaturizing a Microstrip Antenna Using Metamaterials and Metasurfaces,” *IEEE Antennas and Propagation Magazine,* **61**, 1, February 2019, pp. 91-135, doi: 10.1109/ MAP.2018.2883018.

4. S. A. H. Saghanezhad and Z. Atlasbaf, “Miniaturized dual-band CPW-fed antenna loaded with U-shaped Metamaterials,” *IEEE Antennas Wireless Propag. Lett.,* **14**, December 2014, pp. 658–661, doi: 10.1109/LAWP. 2014.2376554

5. H. Xu, G. Wang, J. Liang, M. Q. Qi and X. Gao, "Compact Circularly Polarized Antennas Combining Meta-Surfaces and Strong Space-Filling Meta-Resonators," in *IEEE Transactions on Antennas and Propagation*, **61**, 7, July 2013, pp. 3442-3450, doi: 10.1109/TAP.2013.2255855.

6. Y. H. Liu, and X. P. Zhao, “Perfect absorber metamaterial for designing low-RCS patch antenna”,

IEEE Antennas Wireless Propag. Lett. **13**, July, 2014, pp. 1473-1476, doi: 10.1109/LAWP.2014.2341299.

7. Y. Zhang, W. Hong, C. Yu, Z. Kuai, Y. Don and J. Zhou, "Planar Ultra-wideband Antennas With Multiple Notched Bands Based on Etched Slots on the Patch and/or Split Ring Resonators on the Feed Line," in *IEEE Transactions on Antennas and Propagation*, **56**, 9, Sept. 2008, pp. 3063-3068, doi: 10.1109/TAP.2008.928815.

8. S. Bhattacharyya, S. Ghosh, & K. V. Srivastava, "A Wideband Cross Polarization Conversion using Metasurface", *Radio Science*, **52**, 11, November 2017, pp. 1395-1404, doi: 10.1002/2017RS006396.

9. R. M. Hashmi, B. A. Zeb and K. P. Esselle, "Wideband High-Gain EBG Resonator Antennas with Small Footprints and All-Dielectric Superstructures," in *IEEE Transactions on Antennas and Propagation*, **62**, 6, June 2014, pp.2970-2977. doi: 10.1109/TAP.2014.2314534.

10. Y. Zheng *et al*., "Wideband Gain Enhancement and RCS Reduction of Fabry–Perot Resonator Antenna with Chessboard Arranged Metamaterial Superstrate," in *IEEE Transactions on Antennas and Propagation*, **66**, 2, February 2018, pp. 590-599. doi:10.1109/TAP.2017. 2780896.

11. H. Attia, L. Yousefi and O. M. Ramahi, "Analytical model for calculating the radiation field of microstrip antennas with artificial magnetic superstrates: Theory and experiment", *IEEE Transaction Antennas Propagation*, **59**, 5, May 2011, pp. 1438–1445, doi: 10.1109/TAP.2011. 2122295.

12. D. Samantaray, S. Bhattacharyya, & K. V. Srinivas, "A modified fractal-shaped slotted patch antenna with defected ground using metasurface for dual band applications", *International Journal of RF and Microwave Computer-Aided Engineering,* **29**, 12, August 2019, pp. e21932, doi:10.1002/mmce.21932.

13. C. Caloz, T. Itoh, *Electromagnetic Metamaterials: Transmission Line Theory and Microwave Applications*, 2006 John Wiley & Sons, Inc.

14. Saha, C., Siddiqui, J. Y., & Antar, Y. (2019). *Multifunctional Ultra-Wideband Antennas: Trends, Techniques and Applications,* 6000 Broken Sound Parkway, USA, NW: Taylor and Francis.

15. Y.-M. Pan, K. W. Leung, and K. Lu, "Compact quasi-isotropic dielectric resonator antenna with small ground plane", *IEEE Transaction Antennas Propagation*, **62**, 2, Feb. 2014, pp. 577–585, doi:10.1109/TAP.2013.2292082.

16. C. Deng, Y. Li, Z. Zhang, and Z. Feng, "A wideband isotropic radiated planar antenna using sequential rotated L-shaped monopoles", *IEEE Transaction Antennas Propagation,* **62**, 3, March 2014, pp. 1461–1464, doi:10.1109/TAP.2013.2293787.

17. D. Samantaray and S. Bhattacharyya, "A Gain-Enhanced Slotted Patch Antenna Using Metasurface as Superstrate Configuration," *IEEE Transactions on Antennas and Propagation*, **68**, 9, Sept. 2020, pp. 6548-6556, doi: 10.1109/TAP.2020.2990280.

18. S. K. Ghosh, V. S. Yadav, S. Das and S. Bhattacharyya, "Tunable Graphene-Based Metasurface for Polarization- Independent Broadband Absorption in Lower Mid-Infrared (MIR) Range," in *IEEE Transactions on Electromagnetic Compatibility*, March 2019, pp. 1-9, doi: 10.1109/TEMC. 2019.2900757.

19. Nilotpal, Nama, L., Bhattacharyya, S., & Chakrabarti, P., "A metasurface-based broadband quasi nondispersive cross polarization converter for far infrared region," *International Journal of RF and Microwave Computer-Aided Engineering*, **29**, 10, October 2019, pp. 1-9, doi:10.1002/mmce.21889

20. CST Studio Suite- User's Manual, Comput. Simul. Technol., Darmstadt, Germany, 2017.